Terahertz emitters and detectors based on carbon nanotubes

M.E. Portnoi[*]

School of Physics, University of Exeter, Stocker Road, Exeter EX4 4QL, United Kingdom and
International Center for Condensed Matter Physics,
University of Brasilia, 70904-970 Brasilia DF, Brazil

O.V. Kibis[†]

Department of Applied and Theoretical Physics, Novosibirsk State Technical University, Novosibirsk 630092, Russia and
International Center for Condensed Matter Physics,
University of Brasilia, 70904-970 Brasilia DF, Brazil

M. Rosenau da Costa[‡]

International Center for Condensed Matter Physics,
University of Brasilia, 70904-970 Brasilia DF, Brazil

(Dated: 28 August, 2006)

We formulate and justify several proposals utilizing the unique electronic properties of different types of carbon nanotubes for a broad range of applications to THz optoelectronics, including THz generation by hot electrons in quasi-metallic nanotubes, frequency multiplication in chiral-nanotube-based superlattices controlled by a transverse electric field, and THz radiation detection and emission by armchair nanotubes in a strong magnetic field.

I. INTRODUCTION

Creating a compact reliable source of terahertz (THz) radiation is one of the most formidable tasks of the contemporary applied physics.[1] One of the latest trends in THz technology[2] is to use carbon nanotubes — cylindrical molecules with nanometer diameter and micrometer length[3,4,5,6] — as building blocks of novel high-frequency devices. There are several promising proposals of using carbon nanotubes for THz applications including a nanoklystron utilizing extremely efficient high-field electron emission from nanotubes,[2,7] devices based on negative differential conductivity in large-diameter semiconducting nanotubes,[8,9] high-frequency resonant-tunneling diodes[10] and Schottky diodes,[11,12,13,14] as well as electric-field-controlled carbon nanotube superlattices,[15] frequency multipliers,[16,17] THz amplifiers,[18] switches[19] and antennas.[20]

In this Paper we will formulate and discuss several novel schemes to utilize physical properties of single-wall carbon nanotubes (SWNTs) for generation and detection of THz radiation.

II. QUASI-METALLIC CARBON NANOTUBES AS TERAHERTZ EMITTERS

In this Section we propose a novel scheme for generating THz radiation from single-walled carbon nanotubes (SWNTs). This scheme is based on the electric-field induced heating of electron gas resulting in the inversion of population of optically active states with the energy difference within the THz spectrum range. It is well-known that the elastic backscattering processes in metallic SWNTs are strongly suppressed,[21] and in a high enough electric field charge carriers can be accelerated up to the energy allowing emission of optical/zone-boundary phonons. At this energy, corresponding to the frequency of about 40 THz, the major scattering mechanism switches on abruptly resulting in current saturation.[22,23,24,25,26] In what follows we show that for certain types of carbon nanotubes the heating of electrons to the energies below the phonon-emission threshold results in the spontaneous THz emission with the peak frequency controlled by an applied voltage.

The electron energy spectrum of metallic SWNTs $\varepsilon(k)$ linearly depends on the electron wave vector k close to the Fermi energy and has the form $\varepsilon(k) = \pm \hbar v_F |k - k_0|$, where $v_F \approx 9.8 \times 10^5$ m/s is the Fermi velocity of graphene, which corresponds to the commonly used tight-binding matrix element $\gamma_0 = 3.033$ eV.[4,5,6] Here and in what follows the zero of energy is defined as the Fermi energy position in the absence of an external field. When the voltage, V, is applied between the SWNT ends, the electron distribution is shifted in the way shown by the heavy lines in Fig. 1 corresponding to the filled electron states. This shift results in inversion of population and, correspondingly, in optical transitions between filled states in the conduction band and empty states in the valence band. The spectrum of optical transitions is determined by the distribution function for hot carriers, which in turn depends on the applied
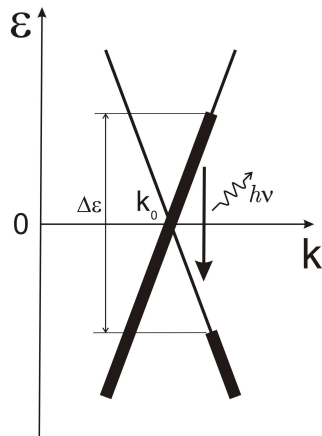
FIG. 1: The scheme of THz photon generation by hot carriers in metallic SWNTs.

voltage and scattering processes in the SWNT. It is well-known that the major scattering mechanism in SWNTs is due to electron-phonon interaction.[22,23,24,26] Since the scattering processes erode the inversion of electron population, an optimal condition for observing the discussed optical transitions takes place when the length of the SWNT $L < l_{ac}$, where the electron mean-free path for acoustic phonon scattering is $l_{ac} \approx 2.4$ μm.[24] Below we consider only such short SWNTs with ideal Ohmic contacts[23] and in the ballistic transport regime, when the energy acquired by the electron on the whole length of the tube, $\Delta\varepsilon = eV$, does not exceed the value of $\hbar\Omega = 0.16$ eV at which the fast emission of high-energy phonons begins.[24] In this regime,[23,24] the current in the nanotube is given by the Büttiker-Landauer formula, $I \approx (4e^2/h)V$, and the distribution function for hot electrons is

$$f_e(k) = \begin{cases} 1, & 0 < k - k_0 < \Delta\varepsilon/2\hbar v_F \\ 0, & k - k_0 > \Delta\varepsilon/2\hbar v_F \end{cases}. \tag{1}$$

The distribution function for hot holes, $f_h(k)$, has the same form as $f_e(k)$.

Let us select a SWNT with the crystal structure most suitable for observation of the discussed effect. First, the required nanotube should have metallic conductivity and, second, the optical transitions between the lowest conduction subband and the top valence subband should be allowed. The crystal structure of a SWNT is described by two integers (n, m), which completely define their physical properties.[3,4,5,6] The SWNTs with true metallic energy band structure, for which the energy gap is absent for any SWNT radius, are the armchair (n, n) SWNTs only.[6,27,28,29,30] However, for armchair SWNTs the optical transitions between the first conduction and valence subbands are forbidden.[31,32] So we propose to use for the observation of THz generation the so-called quasi-metallic (n, m) SWNTs with $n - m = 3p$, where p is an non-zero integer. These nanotubes, which are gapless within the frame of a simple zone-folding model of the π-electron graphene spectrum,[4] are in fact narrow-gap semiconductors due to curvature effects. Their bandgap is given by[27,30]

$$\varepsilon_g = \frac{\hbar v_F a_{\text{C-C}} \cos 3\theta}{8R^2}, \tag{2}$$

where $a_{\text{C-C}} = 1.42$ Å is the nearest-neighbor distance between two carbon atoms, R is the nanotube radius, and $\theta = \arctan[\sqrt{3}m/(2n + m)]$ is the chiral angle.[4] It can be seen from Eq. (2) that the gap is decreasing rapidly with increasing the nanotube radius. For large values of R this gap can be neglected even in the case of moderate applied voltages due to Zener tunneling of electrons across the gap. It is easy to show in the fashion similar to the original Zener's work[33] that the tunneling probability in quasi-metallic SWNTs is given by $\exp(-\alpha\varepsilon_g^2/eE\hbar v_F)$, where α is a numerical factor close to unity.[34] For example, for a zigzag $(30, 0)$ SWNT the gap is $\varepsilon_g \approx 6$ meV and the Zener breakdown takes place for the electric field $E \sim 10^{-1}$ V/μm, which corresponds to a typical voltage of 0.1 V between
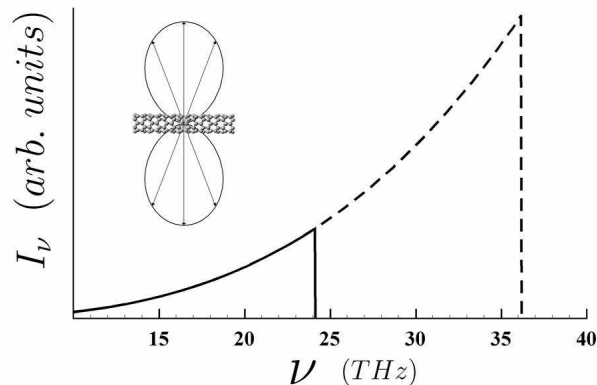
FIG. 2: The spectral density of spontaneous emission as a function of frequency for two values of applied voltage: solid line for $V = 0.1$ V; dashed line for $V = 0.15$ V. The inset shows the directional radiation pattern of the THz emission with respect to the nanotube axis.

the nanotube ends. In what follows all our calculations are performed for a zigzag $(3p, 0)$ SWNT of large enough radius R and for applied voltages exceeding the Zener breakdown, so that the finite-gap effects can be neglected. The obtained results can be easily generalized for any quasi-metallic large-radius SWNT.

Optical transitions in SWNTs have been a subject of extensive research (see, e.g., Refs. 31,32,35,36,37,38,39; comprehensive reviews of the earlier work can be found in Refs. 4,5). We treat these transitions using the results of the nearest-neighbor orthogonal π-electron tight binding model.[4] Despite its apparent simplicity and well-known limitations, this model has been extremely successful in describing low-energy optical spectra and electronic properties of single-walled SWNTs (see, e.g., Ref. 40 for one of the most recent manifestations of this model success). Our goal is to calculate the spectral density of spontaneous emission, I_ν, which is the probability of optical transitions per unit time for the photon frequencies in the interval $(\nu, \nu + d\nu)$ divided by $d\nu$. In the dipole approximation[41] this spectral density is given by

$$I_\nu = \frac{8\pi e^2 \nu}{3c^3} \sum_{i,f} f_e(k_i) f_h(k_f) \left| \langle \Psi_f | \hat{v}_z | \Psi_i \rangle \right|^2 \delta(\varepsilon_i - \varepsilon_f - h\nu). \tag{3}$$

Equation (3) contains the matrix element of the electron velocity operator. In the frame of the tight binding model, this matrix element for optical transitions between the lowest conduction and the highest valence subbands of the $(3p, 0)$ zigzag SWNT can be written as (cf. Ref. 32,35)

$$\langle \Psi_f | \hat{v}_z | \Psi_i \rangle = \frac{a_{\text{C-C}} \omega_{if}}{8} \delta_{k_f, k_i}, \tag{4}$$

where $\hbar \omega_{if} = \varepsilon_i - \varepsilon_f$ is the energy difference between the initial (i) and the final (f) states. These transitions are associated with the light polarized along the nanotube axis z, in agreement with the general selection rules for SWNTs.[31] Substituting Eq. (4) in Eq. (3) and performing necessary summation, we get

$$I_\nu = L f_e(\pi \nu / v_F) f_h(\pi \nu / v_F) \frac{\pi^2 e^2 a_{\text{C-C}}^2 \nu^3}{6 c^3 \hbar v_F}. \tag{5}$$

Equation (5) has broader applicability limits than the considered case of $L < l_{ac}$ and $eV < \hbar\Omega$, in which the distribution functions for electrons and holes are given by Eq. (1). In the general case there is a strong dependence of I_ν on the distribution functions, which have to be calculated taking into account all the relevant scattering mechanisms.[22,23,24,26] In the discussed ballistic regime the spectral density has a universal dependence on the applied voltage and photon frequency for all quasi-metallic SWNTs. In Fig. 2 the spectral density is shown for two values of the voltage. It is clearly seen that the maximum of the spectral density of emission has strong voltage dependence and lies in the THz frequency range for experimentally attainable voltages. The directional radiation pattern, shown in the inset of Fig. 2, reflects the fact that the emission of light polarized normally to the nanotube axis is forbidden by the selection rules for the optical transitions between the lowest conduction subband and the top valence subband.

For some device applications it might be desirable to emit photons propagating along the nanotube axis, which is possible in optical transitions between the SWNT subbands characterized by angular momenta differing by one.[6,31] To achieve the emission of these photons by the electron heating, it is necessary to have an intersection of such

subbands within the energy range accessible to electrons accelerated by attainable voltages. From our analysis of different types of SWNTs, it follows that the intersection is possible, e.g., for the lowest conduction subbands in several semiconducting zigzag nanotubes and in all armchair nanotubes. However, for an effective THz emission from these nanotubes it is necessary to move the Fermi level very close to the subband intersection point.[42] Therefore, obtaining the THz emission propagating along the nanotube axis is a much more difficult technological problem comparing to the generation of the emission shown in Fig. 2.

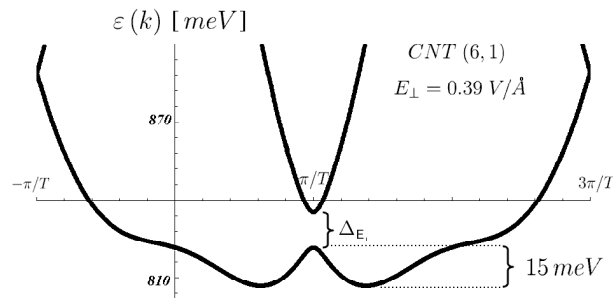### III. CHIRAL CARBON NANOTUBES AS FREQUENCY MULTIPLIERS

FIG. 3: Energy spectrum of the $(6,1)$ SWNT in a transverse electric field, $E_\perp = 4$ V/nm.

Chiral nanotubes are natural superlattices. For example, a $(10,9)$ single-wall nanotube has a radius which differs from the radius of the most commonly studied $(10,10)$ nanotube by less than five per cent, whereas a translational period along the axis of the $(10,9)$ SWNT is almost thirty times larger than the period of the $(10,10)$ nanotube. Correspondingly, the first Brillouin zone of the $(10,9)$ nanotube is almost thirty times smaller than the first zone for the $(10,10)$ tube. However such a Brillouin zone reduction cannot influence electronic transport unless there is a gap opening between the energy subbands resulting from the folding of graphene spectrum. In our research we show how an electric field normal to the nanotube axis opens noticeable gaps at the edge of the reduced Brillouin zone, thus turning a long-period nanotube of certain chirality into a 'real' superlattice. The field-induced gaps are most pronounced in $(n,1)$ SWNTs.[15,43] Figure 3 shows the opening of electric-field induced gap near the edge of the Brillouin zone of a $(6,1)$ SWNT. This gap opening results in the appearance of a negative effective-mass region in
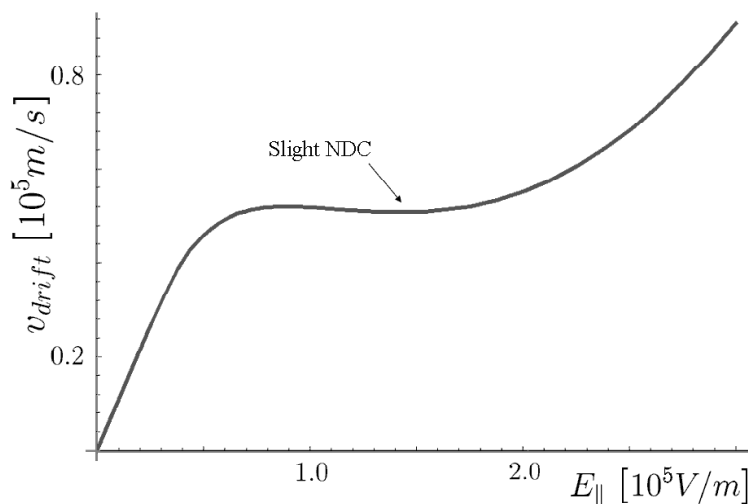

FIG. 4: The electron drift velocity in the lowest conduction subband of a $(6,1)$ SWNT as a function of the longitudinal electric field, in the presence of acoustic phonons.

the nanotube energy spectrum. The typical electron energy in this part of the spectrum of 15 meV is well below the optical phonon energy $\hbar\Omega \approx 160$ meV, so that it can be easily accessed in moderate heating electric fields. The

negative effective mass results in the negative differential conductivity in a wide range of applied voltages, as can be seen from Fig. 4.

The effect of the negative effective mass also leads to an efficient frequency multiplication in the THz range. The results of our calculations of the electron velocity in the presence of the time dependent longitudinal electric field are presented in Fig. 5. One of the advantages of a frequency multiplier based on chiral SWNTs, in comparison with the
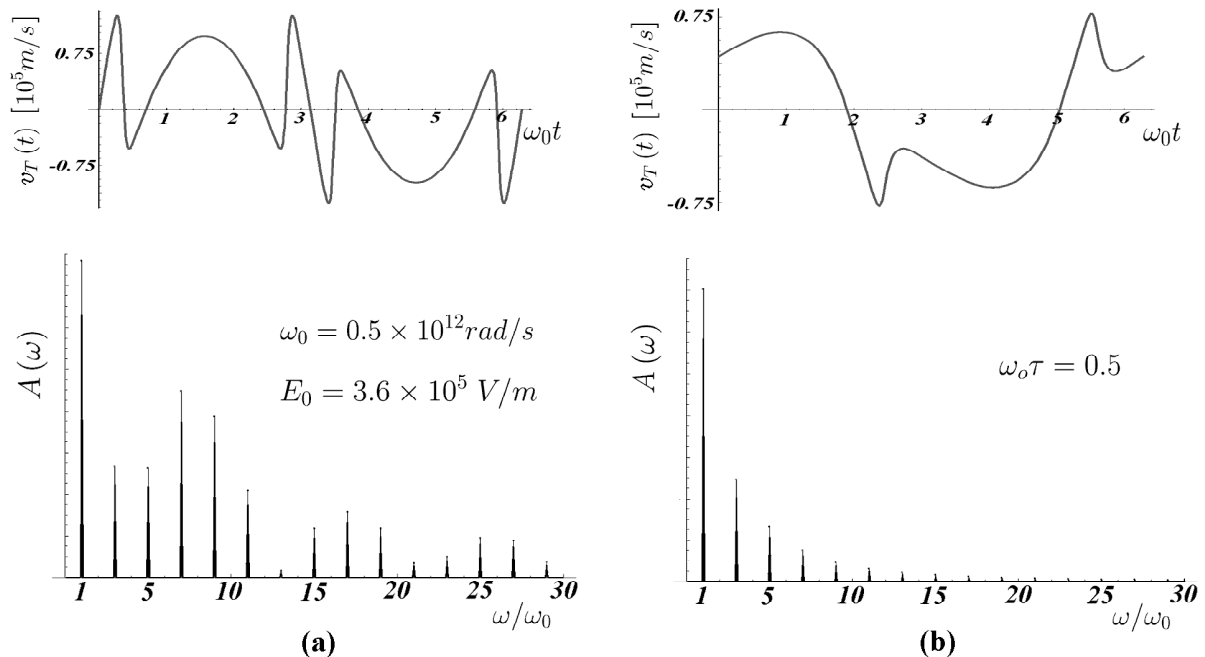

FIG. 5: Time dependence of the electron velocity in the lowest conduction subband of a $(6, 1)$ SWNT under the influence of a pump harmonic longitudinal electric field, $E_\parallel(t) = E_0 \sin(\omega_0 t)$, and its correspondent spectral distribution $A(\omega)$: (a) in the ballistic transport regime; (b) in the presence of scattering with the relaxation time $\tau = 10^{-12} s$.

conventional superlattices,[44] is that the dispersion relation in our system can be controlled by the transverse electric field $E_\perp$.

IV. ARMCHAIR NANOTUBES IN A MAGNETIC FIELD AS TUNABLE THZ DETECTORS AND EMITTERS

The problem of detecting THz radiation is known to be at least as challenging as creating reliable THz sources. Our proposal of a novel detector is based on several features of the truly gapless (armchair) SWNTs. The main property to be utilized is the opening of the gap in these SWNTs in a magnetic field along the nanotube axis[5]. For a $(10, 10)$ SWNT this gap is approximately 1.6 THz in the field of 10 T. For attainable magnetic fields, the gap grows linearly with increasing both magnetic field and the nanotube radius. It can be shown[43] that the same magnetic field also allows dipole optical transitions between the top valence subband and the lowest conduction subband, which are strictly forbidden in armchair SWNTs without the field.[31]

In Figure 6 we show how the energy spectrum and the matrix elements of the dipole optical transitions polarized along the nanotube axis are modified in the presence of a longitudinal magnetic field. In the frame of the nearest-neighbor tight binding model, one can show that for a (n, n) armchair nanotube the squared matrix element of the velocity operator between the states at the edge of the gap opened by the magnetic field is given by a simple analytic expression:

$$|\langle \Psi_n^v |\hat{v}_z| \Psi_i^c \rangle|^2 = \frac{4}{3} \left[1 - \frac{1}{4} \cos^2 \left(\frac{f}{n}\pi \right) \right] v_F^2, \tag{6}$$

where $f = eBR^2/(2\hbar)$. For experimentally attainable magnetic fields, when the magnetic flux through the SWNT is much smaller than the flux quantum, the absolute value of the velocity operator is close to v_F. Equation (6) is relevant to the transitions between the highest valence subband and the the lowest conduction subband only for $f \leq 1/2$, since
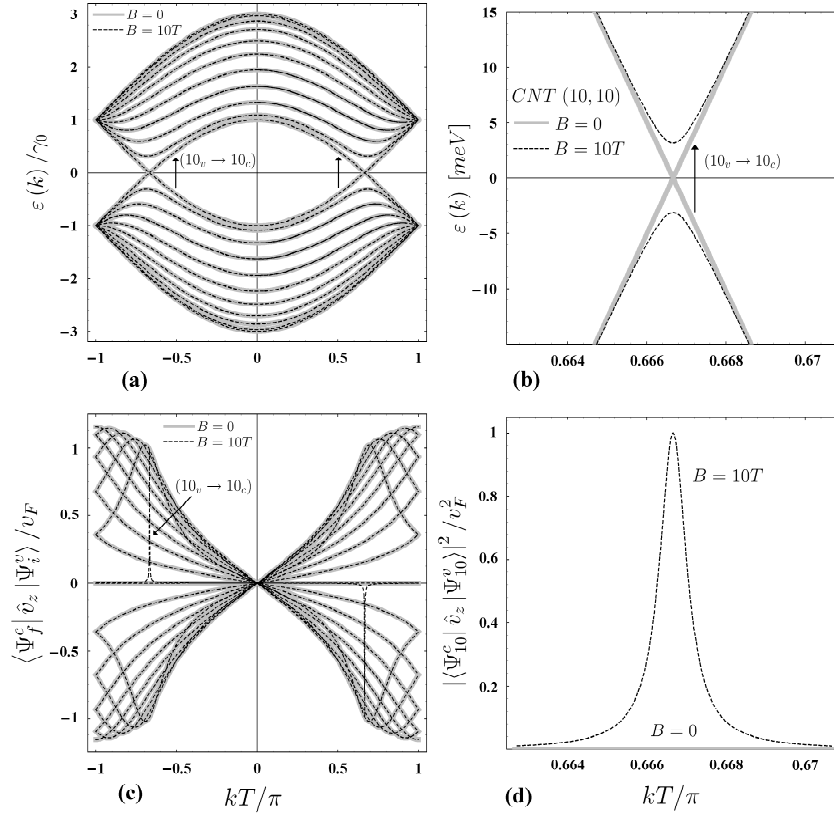
FIG. 6: (a) Band structure of a $(10, 10)$ nanotube, with and without an external magnetic field along the nanotube axis. (b) Detailed view of the gap, which is opened between the top valence subband and the lowest conduction subband in an external field $B = 10$ T. (c) The change in the dipole optical transitions matrix elements, for the light polarized along the SWNT axis, due to the introduction of the external magnetic field. The only appreciable change is in the appearance of a high narrow peak associated with the transition $(10_v \rightarrow 10_c)$, which is not allowed in the absence of the magnetic field. (d) Dependence of the squared dipole matrix element for the transition $(10_v \rightarrow 10_c)$ on the 1D wave vector k, with and without an external magnetic field.

for the higher values of f the order of the nanotube subbands is changed. Notably, the same equation allows to obtain the maximum value of the velocity operator in any armchair SWNT for the transitions polarized along its axis: this value cannot exceed $2v_F/\sqrt{3}$ (see Fig. 6c).
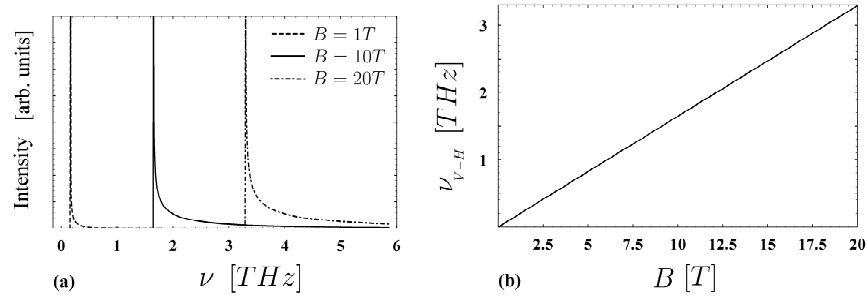

FIG. 7: (a) Calculated photon absorption spectra for a $(10, 10)$ SWNT, for three different magnetic field values. The absorption intensity is proportional to the product of $|\langle \Psi_{10}^v | \hat{v}_z | \Psi_{10}^c \rangle|^2$ and the joint density of states. (b) Dependence of the position of the peak in the absorption intensity, associated with the Van Hove singularity, on the magnetic field.

The electron (hole) energy spectrum near the bottom (top) of the gap produced by the magnetic field is parabolic as a function of a carrier momentum along the nanotube axis. This dispersion results in a Van Hove singularity in
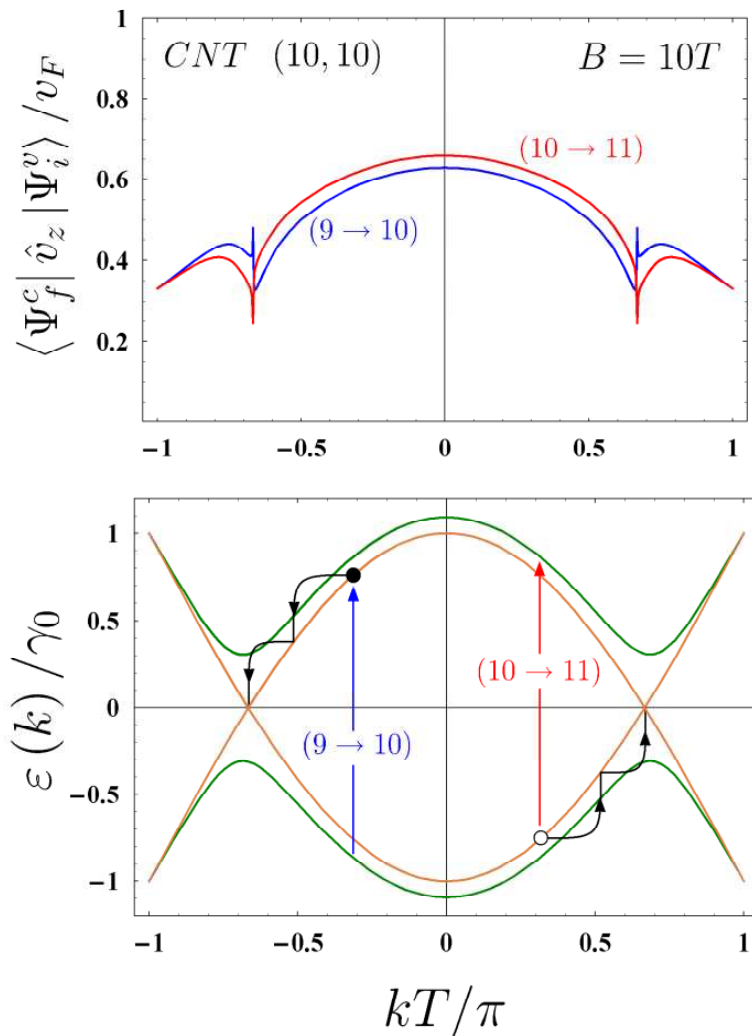
FIG. 8: A scheme for creating a population inversion between the lowest conduction subband and the top valence subband of an armchair SWNT in a magnetic field. The upper plot shows the calculated matrix elements of the relevant dipole optical transitions polarized normally to the axis of a $(10, 10)$ SWNT. The lower plot shows several energy subbands closest to the Fermi level and illustrates the creation of photoexcited carriers and their non-radiative thermalization.

the reduced density of states, which in turn leads to a very sharp absorption maximum near the band edge and, correspondingly, to a very high sensitivity of the photocurrent to the photon frequency, see Fig. 7.

Notably, the same effect can be used for the generation of a very narrow emission line having the peak frequency tunable by the applied magnetic field. A population inversion can be achieved, for example, by optical pumping with the light polarized normally to the nanotube axis, as shown in Fig. 8.

V. CONCLUSIONS

We have demonstrated that a quasi-metallic carbon nanotube can emit the THz radiation when the potential difference is applied to its ends. The typical required voltages and nanotube parameters are similar to those available in the state-of-the-art transport experiments. The maximum of the spectral density of emission is shown to have the strong voltage dependence, which is universal for all quasi-metallic carbon nanotubes in the ballistic regime. Therefore, the discussed effect can be used for creating a THz source with the frequency controlled by the applied voltage. Appropriately arranged arrays of the nanotubes should be considered as promising candidates for active elements of amplifiers and generators of the coherent THz radiation.

We have also shown that an electric field, which is applied normally to the axis of long-period chiral nanotubes,

significantly modifies their band structure near the edge of the Brillouin zone. This results in the negative effective mass region at the energy scale below the high-energy phonon emission threshold. This effect can be used for an efficient frequency multiplication in the THz range.

Finally, we have discussed the feasibility of using the effect of the magnetic field, which opens the energy gaps and allows optical transitions in armchair nanotubes, for tunable THz detectors and emitters.

Acknowledgments

[*] m.e.portnoi@exeter.ac.uk

[†] oleg.kibis@nstu.ru

[‡] rosenau@unb.br

[1] B. Ferguson and X.C. Zhang, "Materials for terahertz science and technology", *Nature Materials* **1**, pp. 26–33, 2002.

[2] D. Dragoman and M. Dragoman, "Terahertz fields and applications", *Progress in Quantum Electronics* **28**, pp. 1–66, 2004.

[3] S. Iijima, "Helical microtubules of graphitic carbon", *Nature* **354**, pp. 56–58, 1991.

[4] R. Saito, G. Dresselhaus, and M.S. Dresselhaus, *Physical Properties of Carbon Nanotubes*, Imperial College Press, London, 1998.

[5] *Carbon Nanotubes: Synthesis, Structure, Properties, and Applications*, edited by M.S. Dresselhaus, G. Dresselhaus, and Ph. Avouris, Springer-Verlag, Berlin, 2001.

[6] S. Reich, C. Thomsen, and J. Maultzsch, *Carbon Nanotubes: Basic Concepts and Physical Properties*, Wiley, Berlin, 2004.

[7] H.M. Manohara, M.J. Bronikowski, M. Hoenk, B.D. Hunt, and P.H. Siegel, "High-current-density field emitters based on arrays of carbon nanotube bundles", *J. Vac. Sci. Technol. B* **23**, pp. 157–161, 2005.

[8] A.S. Maksimenko and G.Ya. Slepyan, "Negative differential conductivity in carbon canotubes", *Phys. Rev. Lett.* **84**, pp. 362–365, 2000.

[9] G. Pennington and N. Goldsman, "Semiclassical transport and phonon scattering of electrons in semiconducting carbon nanotubes", *Phys. Rev. B*, **68**, p. 045426, 2003.

[10] D. Dragoman and M. Dragoman, "Terahertz oscillations in semiconducting carbon nanotube resonant-tunneling diodes", *Physica E* **24**, pp. 282–289, 2004.

[11] A.A. Odintsov, "Schottky Barriers in Carbon Nanotube Heterojunctions ", *Phys. Rev. Lett.* **85**, pp. 150–153, 2000.

[12] F. Léonard and J. Tersoff, "Negative Differential Resistance in Nanotube Devices", *Phys. Rev. Lett.* **85**, pp. 4767–4770, 2000.

[13] M.H. Yang, K.B.K. Teo, W.I. Milne, and D.G. Hasko, "Carbon nanotube Schottky diode and directionally dependent field-effect transistor using asymmetrical contacts", *Appl. Phys. Lett.* **87**, p. 253116, 2005.

[14] C. Lu, L. An, Q. Fu, J. Liu, H. Zhang, and J. Murduck, "Schottky diodes from asymmetric metal-nanotube contacts", *Appl. Phys. Lett.* **88**, p. 133501, 2006.

[15] O.V. Kibis, D.G.W. Parfitt, and M.E. Portnoi, "Superlattice properties of carbon nanotubes in a transverse electric field", *Phys. Rev. B* **71**, pp. 035411, 2005.

[16] G.Ya. Slepyan, S.A. Maksimenko, V.P. Kalosha, J. Herrmann, E.E.B. Campbell, and I.V. Hertel, "Highly efficient high-order harmonic generation by metallic carbon nanotubes", *Phys. Rev. A* **60**, pp. 777–780, 1999. (1999).

[17] G.Ya. Slepyan, S.A. Maksimenko, V.P. Kalosha, A.V. Gusakov and J. Herrmann, Phys. Rev. A **63**, 053808 (2001).

[18] D. Dragoman, M. Dragoman, "Terahertz continuous wave amplification in semiconductor carbon nanotubes", *Physica E* **25**, pp. 492–496, 2005.

[19] M. Dragoman, A. Cismaru, H. Hartnagel, and R. Plana, "Reversible metal-semiconductor transitions for microwave switching applications", *Appl. Phys. Lett.* **88**, p. 073503, 2006.

[20] G.Ya. Slepyan, M.V. Shuba, S.A. Maksimenko, and A. Lakhtakia, "Theory of optical scattering by achiral carbon nanotubes and their potential as optical nanoantennas", *Phys. Rev. B* **73**, p. 195416, 2006.

[21] T. Ando, T. Nakanishi, and R. Saito, "Impurity scattering in carbon nanotubes — absence of back scattering", *J. Phys. Soc. Jpn.* **67**, pp. 1704–1713, 1997.

[22] Z. Yao, C.L. Kane, and C. Dekker, "High-field electrical transport in single-wall carbon nanotubes", *Phys. Rev. Lett.* **84**, pp. 2941–2944, 2000.

[23] A. Javey, J. Guo, M. Paulsson, Q. Wang, D. Mann, M. Lundstrom, and H. Dai, "High-Field Quasiballistic Transport in Short Carbon Nanotubes", *Phys. Rev. Lett.* **92**, p. 106804, 2004.

[24] J.-Y. Park, S. Resenblatt, Yu. Yaish, V. Sazonova, H. Üstünel, S. Braig, T.A. Arias, P.W. Brouwer, and P.L. McEuen, "Electron-phonon scattering in metallic single-walled carbon nanotubes", *Nano Lett.* **4**, pp. 517–520, 2004.

[25] M. Freitag, V. Pereibenos, J. Chen, A. Stein, J.c. Tsang, J.A. Misewich, R. Martel, and Ph. Avouris, "Hot carrier electroluminescence from a single carbon nanotube", *Nano Lett.* **4**, pp. 1063–1066, 2004.

[26] V. Perebeinos, J. Tersoff, and P. Avouris, "Electron-phonon interaction and transport in semiconducting carbon nanotubes", *Phys. Rev. Lett.* **94**, p. 086802, 2005.

[27] C.L. Kane and E.J. Mele, "Size, shape, and low energy electronic structure of carbon nanotubes", *Phys. Rev. Lett.* **78**, pp. 1932–1935, 1997.

[28] M. Ouyang, J.-L. Huang, C.L. Cheung, and C.M. Lieber, "Energy gaps in "metallic" single-walled carbon nanotubes", *Science* **292**, pp. 702–705, 2001.

[29] Y. Li, U. Ravaioli, and S.V. Rotkin, "Metal-semiconductor transition and Fermi velocity renormalization in metallic carbon nanotubes", *Phys. Rev. B* **73**, p. 035415, 2006.

[30] D. Gunlycke, C.J. Lambert, S.W.D. Bailey, D.G. Pettifor, G.A.D. Briggs, and J.H. Jefferson, "Bandgap modulation of narrow-gap carbon nanotubes in a transverse electric field ", *Europhys. Lett.* **73**, pp. 759–764, 2006.

[31] I. Milošević, T. Vuković, S. Dmitrović, and M. Damnjanović, "Polarized optical absorption in carbon nanotubes: A symmetry-based approach", *Phys. Rev. B* **67**, p. 165418, 2003.

[32] J. Jiang, R. Saito, A. Grüneis, G. Dresselhaus, and M.S. Dresselhaus, "Optical absorption matrix elements in single-wall carbon nanotubes", *Carbon* **42**, pp. 3169–3176, 2004.

[33] C. Zener, "A theory of the electrical breakdown of solid dielectrics", *Proc. Royal. Soc. (London)* **145**, p. 523, 1934.

[34] For the energy spectrum near the band edge given by $\varepsilon = \pm \left[\varepsilon_g^2/4 + \hbar^2 v_F^2 (k - k_0)^2\right]^{1/2}$, it can be shown that $\alpha = \pi/4$.

[35] A. Grüneis, R. Saito, G.G. Samsonidze, T. Kimura, M.A. Pimenta, A. Joria, A.G. Souza Filho, G. Dresselhaus, and M.S. Dresselhaus, "Inhomogeneous optical absorption around the K point in graphite and carbon nanotubes", *Phys. Rev. B* **67**, p. 165402, 2003.

[36] V.N. Popov and L. Henrard, "Comparative study of the optical properties of single-walled carbon nanotubes within orthogonal and nonorthogonal tight-binding models", *Phys. Rev. B* **70**, p. 115407, 2004.

[37] R. Saito, A. Grüneis, G.G. Samsonidze, G. Dresselhaus, M.S. Dresselhaus, A. Jorio, L.G. Cançado, M.A. Pimenta, and A.G. Souza Filho, "Optical absorption of graphite and single-wall carbon nanotubes", *Appl. Phys. A* **78**, pp. 1099–1105, 2004.

[38] S.V. Goupalov, "Optical transitions in carbon nanotubes", *Phys. Rev. B* **72**, p. 195403, 2005.

[39] Y. Oyama, R. Saito, K. Sato, J. Jiang, G.G. Samsonidze, A. Grüneis, Y. Miyauchi, S. Maruyama, A. Jorio, G. Dresselhaus, and M.S. Dresselhaus, "Photoluminescence intensity of single-wall carbon nanotubes", *Carbon* **44**, pp. 873–879, 2006.

[40] M.Y. Sfeir, T. Beetz, F. Wang, L. Huang, X.M.H. Huang, M. Huang, J. Hone, S. O'Brien, J.A. Misewich, T.F. Heinz, L. Wu, Y. Zhu, L.E. Brus, "Optical spectroscopy of individual single-walled carbon nanotubes of defined chiral structure", *Science* **312**, pp. 554–556, 2006.

[41] V.B. Berestetskii, E.M. Lifshitz, and L.P. Pitaevskii, *Quantum Electrodynamics*, Butterworth-Heinemann, Oxford, 1997.

[42] O.V. Kibis and M.E. Portnoi, "Carbon nanotubes: A new type of emitter in the terahertz range", *Technical Phys. Lett.* **31**, pp. 671–672, 2005.

[43] M. Rosenau da Costa, O.V. Kibis and M.E. Portnoi, *to be published*.

[44] K.N. Alekseev, M.V. Gorkunov, N.V. Demarina, T. Hyart, N.V. Alexeeva, and A.V. Shorokhov, "Suppressed absolute negative conductance and generation of high-frequency radiation in semiconductor superlattices", *Europhys. Lett.* **73**, pp. 934–940, 2006.